Structural characterization of Group 4 transition metal halide bis-Arduengo carbene complexes MCl4L2:: X-ray crystal structure analyses and DFT calculations

ARTICLE *in* JOURNAL OF ORGANOMETALLIC CHEMISTRY · DECEMBER 2002

Impact Factor: 2.17 · DOI: 10.1016/S0022-328X(02)01731-X

Available online at www.sciencedirect.com
SCIENCE DIRECT®
Journal of Organometallic Chemistry 663 (2002) 192–203
Journal of Organometallic Chemistry
www.elsevier.com/locate/jorganchem

Structural characterization of Group 4 transition metal halide bis-Arduengo carbene complexes MCl_4L_2: X-ray crystal structure analyses and DFT calculations

Martin Niehues [a], Gerald Kehr [a], Gerhard Erker [a,*], Birgit Wibbeling [1,a], Roland Fröhlich [1,a], Olivier Blacque [2,b], Heinz Berke [2,b]

[a] Organisch-Chemisches Institut der Universität Münster, Corrensstrasse 40, D-48149 Münster, Germany
[b] Anorganisch-Chemisches Institut der Universität Zürich, Winterthurer Strasse 190, CH-8057 Zürich, Switzerland

Received 4 June 2002; accepted 18 July 2002

Dedicated to our friend and colleague Professor Pascual Royo on the occasion of his 65th birthday

Abstract

The Arduengo carbenes 1,3-diisopropyl-, 1-methyl-3-(1-methylpropyl)-, and 1-methyl-3-(2,4,6-trimethylbenzyl)imidazol-2-ylidene (**3a**–**c**) were reacted with $MCl_4(thf)_2$ (M = Zr, Hf) to yield the respective *trans*-(imidazol-2-ylidene)MCl_4 complexes **4a**–**c** (M = Zr) and **5a** (M = Hf), respectively. These four Arduengo carbene-Group 4 metal halide complexes were characterized by X-ray diffraction. The pairs of carbene ligands are *trans*-positioned in a pseudo-octahedral coordination geometry at the Group 4 metals, and adopt a conformational orientation in the solid state where the two five-membered heterocycles are arranged coplanar and bisecting the Cl–M–Cl angle. DFT calculations have shown that the Arduengo carbenes serve as pure σ-donor ligands in these complexes and that the preferred conformational ligand orientation is based on steric reasons. The complexes **4a**–**c** form moderately active ethene polymerization catalysts when activated with a large excess of methylalumoxane in toluene.

Keywords: Arduengo carbenes; d°-Metal complexes; DFT calculation; X-ray crystal structure analyses; Ethene polymerization

1. Introduction

The stable *N*-heterocyclic 'Arduengo carbenes' [1] have found a wide application in organometallic chemistry and catalysis [2,3]. They are powerful σ-donor ligands, but they exhibit almost negligible π-acceptor properties. Especially the *N*-alkyl- or *N*-aryl-substituted imidazol-2-ylidenes have been employed as ligands for most of the transition metals throughout the periodic table [1,2,4], but surprisingly few examples of Group 4 metal complexes with 'Arduengo carbene ligands' have been described and characterized by X-ray diffraction so far.

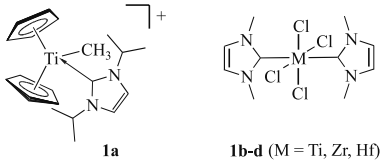

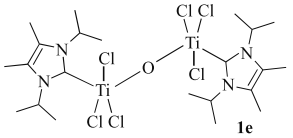

We have recently published [5] the preparation and X-ray crystal structure analysis of the salt $[Cp_2TiCH_3(1,3\text{-diisopropylimidazol-2-ylidene})^+][BPh_4^-]$ (**1**), to our knowledge first example of an alkyl-metallocene–Arduengo carbene cation complex, that

* Corresponding author. Tel.: +49-251-8333221; fax: +49-251-8336503
E-mail address: erker@uni-muenster.de (G. Erker).
[1] X-ray crystal structure analyses.
[2] DFT calculations.

0022-328X/02/$ - see front matter
PII: S0022-328X(02)01731-X

was structurally characterized. Herrmann et al. in 1994 described the preparation of the series of [(1,3-dimethylimidazol-2-ylidene)$_2$MCl$_4$] complexes **1** (**b**–**d**, M = Ti, Zr, Hf) [6]. These systems were obtained by treatment of the [MCl$_4$(thf)$_2$] precursors with two molar equivalents of the free heterocyclic carbene. X-ray crystal structure analyses of the complexes **1b**–**d**, were not published in the open literature [7] so far, to our knowledge. Kuhn et al. have published the structure of the μ-oxo-titanium complex **1e** that contains the 1,3-diisopropyl-4,5-dimethylimidazol-2-ylidene ligand coordinated *trans* to the bridging oxygen group at titanium [7].

We here report the preparation and structural characterization of a series of differently substituted [(imidazolyl-2-ylidene)$_2$MCl$_4$] complexes of zirconium and hafnium. These appear to represent the first examples of such systems of these second and third row Group 4 metals that were characterized by X-ray diffraction [8]. In addition, a DFT analysis of the characteristic coordination features of these complexes was carried out, and we have briefly investigated first catalytic properties of these systems.

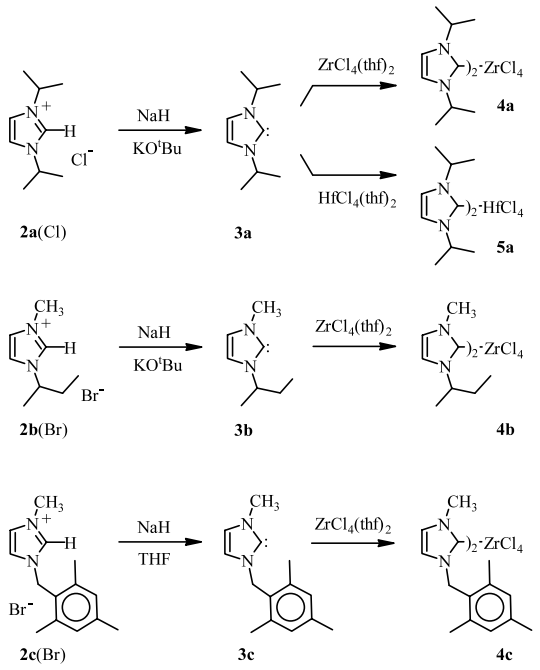

Scheme 1.

2. Results and discussion

2.1. Syntheses and structural characterization

We have used three different stable imidazole-derived carbene ligands for this study. 1,3-Diisopropylimidazolium chloride [**2a**(Cl)] was prepared by a stepwise condensation reaction between isopropylamine, (para)-formaldehyde, and (aqueous) glyoxal as described in the literature [9]. Subsequence deprotonation with NaH–KO^{t}Bu, as described by Arduengo et al. [10] gave 1,3-diisopropyl-imidazol-2-ylidene (**3a**) in 95% yield (see Scheme 1). Treatment of *N*-methylimidazole with 2-bromobutane yielded the imidazolium salt **2b**(Br), which was converted to the stable carbene **3b** (65% isolated) by treatment with NaH–KO^{t}Bu. Finally, the imidazolium salt **2c**(Br), prepared by *N*-alkylation of *N*-methylimidazole with bromomethyl-2,4,6-trimethylbenzene, was converted to the unsymmetrically substituted Arduengo carbene **3c** by treatment with NaH in tetrahydrofuran at ambient temperature.

The complexes **4a**–**c** and **5a** were characterized by X-ray diffraction and spectroscopically. For the purpose of a comparison we have also carried out the X-ray crystal structure analyses of the imidazolium salt **2c**(Br) and the related imidazolium salts **2a**(BPh$_4$) and **2b**(BPh$_4$), respectively. The latter two compounds were prepared by anion exchange from **2a**(Cl) and **2b**(Br), respectively, by treatment with NaBPh$_4$. Details of these imidazolium structures are listed in Table 1 and in Section 3.

The complex bis(1,3-diisopropylimidazol-2-ylidene)-zirconium tetrachloride (**4a**) contains two symmetry equivalent Arduengo carbene ligands. Consequently, these exhibit a single set of ^{1}H- and ^{13}C-NMR resonances. The ligands behave C_{2v}-symmetric in solution. Consequently, they exhibit a single set of isopropyl ^{1}H-/^{13}C-NMR signals and a single C4/C5 resonance [δ 117.4; 4-H/5-H-NMR signals at δ 7.10 (s, 2H)]. The C2 ^{13}C-NMR resonance of **4a** is observed at δ 181.8 (the corresponding C2 signal of the Arduengo carbene precursors are found at much larger δ values, e.g. **3a**: δ 210.5).

The X-ray crystal structure analysis of complex **4a** shows that two 1,3-diisopropylimidazol-2-ylidene ligands were added to the ZrCl$_4$ moiety in a *trans*-arrangement to complete a pseudooctahedral coordination sphere around the central zirconium atom. Due to symmetry the corresponding bond angles at zirconium all amount to the ideal value of 180°: C2–Zr–C2*, Cl1–Zr–Cl1*, Cl2–Zr–Cl2*. The Zr–Cl bond lengths (Zr–Cl1: 2.439(1) Å, Zr–Cl2: 2.437(1) Å) are in the same range as is the Zr–C2 bond length at 2.432(3) Å. The latter is in the general area expected for Zr–C σ-interactions, although located at the high end of the typical range of zirconium–carbon bonds (Zr–CH$_3$ average: 2.292 Å) [10,11]. This clearly indicates the pure σ-donor nature of the imidazol-2-ylidene ligand to zirconium interaction in **4a**, as it is typical for these types of ligands [1,2,5] (Fig. 1).

The bond lengths inside the five-membered heterocyclic ligands of **4a** are considerably equilibrated (see Table 1). The C2–N1 and C2–N3 bonds are almost equal in length (1.367(3) and 1.365(3) Å). The adjacent N3–C4 (1.378(4) Å) and N1–C5 (1.373(4) Å) bonds are

Table 1
Selected structural data of the imidazol-2-ylidene complexes **4a**–**c** and **5a** [a]

Compound	N1–C2	C2–N3	N3–C4	C4–C5	C5–N1	M–C2
4a	1.367(3)	1.365(3)	1.378(4)	1.327(5)	1.373(4)	2.432(3)
5a	1.359(3)	1.361(3)	1.369(4)	1.327(5)	1.376(4)	2.401(2)
4b	1.364(4)	1.363(4)	1.376(5)	1.335(6)	1.368(5)	2.456(3)
4c	1.364(4)	1.369(4)	1.364(4)	1.333(5)	1.376(4)	2.448(3)
2a(BPh_4)	1.324(2)	1.324(2)	1.379(2)	1.350(4)	1.379(2)	–
2b(BPh_4)	1.325(7)	1.316(6)	1.368(8)	1.306(13)	1.382(7)	–
2c(Br)	1.329(3)	1.327(3)	1.371(3)	1.348(3)	1.377(3)	–

Data of the imidazolium salts **2a**(BPh_4), **2b**(BPh_4) and **2c**(Br) are listed for comparison.
[a] Bond lengths in Å.

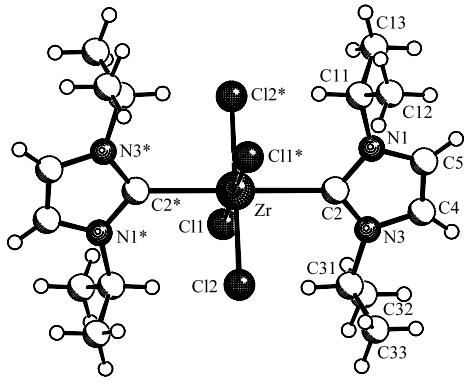

Fig. 1. Molecular structure of **4a**. Selected bond lengths (Å) and angles (°): selected bond lengths and angles for **4a**: Zr–Cl1 2.439(1), Zr–Cl2 2.437(1), Zr–C2 2.432(3), N1–C2 1.367(3), C2–N3 1.365(3), N1–C5 1.373(4), N3–C4 1.378(4), N1–C11 1.481(4), N3–C31 1.482(4), C4–C5 1.327(5); Cl1–Zr–Cl1* 180.0, Cl2–Zr–Cl2* 180.0, C2–Zr–C2* 180.0, Cl1–Zr–Cl2 91.67(3), Cl1–Zr–C2 89.62(7), Cl2–Zr–C2 90.76(7), Zr–C2–N1 127.8(2), Zr–C2–N3 128.7(2), N1–C2–N3 103.3(2), C2–N3–C4 111.1(2), N3–C4–C5 107.1(3), C4–C5–N1 107.4(3), C5–N1–C2 111.2(2), C2–N1–C11 127.0(2), C2–N3–C31 126.3(2).

only slightly longer, but the central C4–C5 linkage is markedly shorter at 1.327(5) Å. Compared to its imidazolium salt precursor (here **2a**(BPh_4), see Table 1) the C2–N1/3 bonds of the heterocyclic ligand in **4a** have become elongated by ca. $\Delta d = 0.04$ Å, whereas the adjacent N3–C4 and N1–C5 bond lengths have remained largely unchanged. This probably points to a considerable steric effect exerted by the bulky $LZrCl_4$ moiety on the adjacent imidazol-2-ylidene ring system in complex **4a**. This view is supported by the observed slight increase of the C2–N–C(isopropyl) angles on going from the imidazolium reference **2a**(BPh_4) (C2–N1–C4: 124.8(2)° to the coordination compound **4a** (C2–N1–C11: 127.0(2)°, C2–N3–C31: 126.3(2)°).

In the crystal the 1,3-diisopropylimidazol-2-ylidene ligands of **4a** have attained a specific conformation. Their five-membered rings are oriented coplanar within the octahedral framework, and the imidazol-2-ylidene planes are arranged bisecting the Cl1–Zr–Cl2 angle at zirconium. This arrangement leaves a maximal separation between the central chloride ligands and the peripheral isopropyl substituents at the nitrogen atoms of the five-membered ring σ-donor ligands in complex **4a**. The corresponding dihedral angles amount to 130.1(3) (N1–C2–Zr–Cl1) and −138.3(2)° (N1–C2–Zr–Cl2).

The hafnium complex **5a** shows an analogous structure. Again the 1,3-diisopropylimidazol-2-ylidene ligands are oriented *trans* to each other within the octahedral coordination geometry and the common imidazol-2-ylidene plane is bisecting the Cl1–Hf–Cl2 angle. The Hf–C2 linkage in **5a** (2.401(2) Å) is by ca. $\Delta d = 0.03$ Å *smaller* than the respective Zr–C2 distance in **4a**. This corresponds to a typical difference of metal–carbon σ-bond lengths between these two Group 4 metals [11] (Fig. 2).

Bis(1-methyl-3-methylpropyl-imidazol-2-ylidene)$ZrCl_4$ (**4b**) shows a similar structure in the crystal. Again the *trans*-carbene ligands are arranged coplanar and bisecting the Cl–Zr–Cl angle. In this arrangement

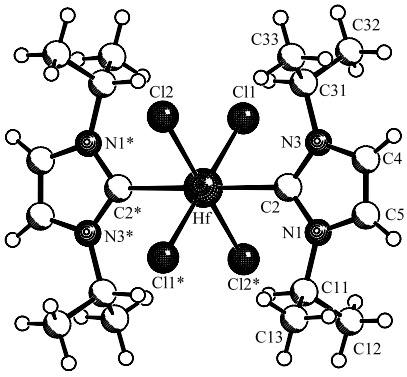

Fig. 2. A view of the molecular structure of the hafnium complex **5a** in the crystal. Selected bond lengths (Å) and angles (°): Hf–Cl1 2.421(1), Hf–Cl2 2.419(1), Hf–C2 2.401(2), N1–C2 1.359(3), C2–N3 1.361(3), N1–C5 1.376(4), N3–C4 1.369(4), N1–C11 1.471(4), N3–C31 1.473(4), C4–C5 1.327(5); Cl1–Hf–Cl1* 180.0, Cl2–Hf–Cl2* 180.0 C2–Hf–C2* 180.0, Cl1–Hf–Cl2 92.06(2), Cl1–Hf–C2 89.70(6), Cl2–Hf–C2 90.75(6), Hf–C2–N1 127.7(2), Hf–C2–N3 128.3(2), N1–C2–N3 104.0(2), C2–N3–C4 110.8(2), N3–C4–C5 107.4(3), C4–C5–N1 107.2(3), C5–N1–C2 110.7(2), C2–N1–C11 127.5(2), C2–N3–C31 126.7(2).

the two bulky *sec*-butyl substituents at the imidazol-2-ylidene nitrogen ligand are oriented *anti* to each other, i.e. placed as to achieve a maximal spatial separation (see Fig. 3).

Complex **4c** features an analogous structural arrangement. The imidazol-2-ylidene ligands in **4c** are oriented *trans*-coplanar and bisected at the $ZrCl_4$ core. The very bulky $-CH_2-$mesityl groups are oriented *anti*- to each other, pointing to the periphery of the complex. The C7–C8 vector in **4c** is rotated by $-39.8(4)^\circ$ (C5–N1–C7–C8) relative to the plane of the five-membered heterocyclic carbene ligand (see Fig. 4).

2.2. DFT calculations

The bonding features of the carbene complexes **4** and related systems were achieved from a theoretical study [12,13]. Recently, we have theoretically investigated [5] the interaction between a neutral imidazol-2-ylidene and a d^0 transition metal fragment Cp_2TiMe^+. It could be shown that the overall bonding situation of the carbene ligand does not correspond to the general picture of Fischer-type carbene complexes, where the metal–carbon interaction consists of a superimposed carbene to metal σ-donation and metal to carbene π-back donation. Specifically for d^0 systems, the carbene to metal interaction would only have σ-donation. Moreover, imidazolylidene carbenes like the Arduengo systems are not well disposed for π-back bonding due to the relatively high-lying vacant p_π-orbital. Thus, in conjunction with d^0 metallocene moieties, such carbenes are expected to serve as only pure σ-donor ligands and we could show earlier that steric influences may become essential for the conformational preference of the

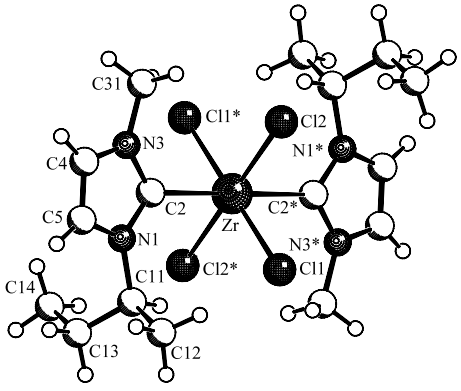

Fig. 3. Molecular structure of **4b**. Selected bond lengths (Å) and angles (°): Zr–Cl1 2.436(1), Zr–Cl2 2.428(1), Zr–C2 2.456(3), N1–C2 1.364(4), C2–N3 1.363(4), N1–C5 1.368(5), N3–C4 1.376(5), N1–C11 1.495(5), N3–C31 1.461(5), C4–C5 1.335(6); Cl1–Zr–Cl1* 180.0, Cl2–Zr–Cl2* 180.0 C2–Zr–C2* 180.0, Cl1–Zr–Cl2 88.16(3), Cl1–Zr–C2 89.48(8), Cl2–Zr–C2 88.35(8), Zr–C2–N1 129.1(2), Zr–C2–N3 127.2(2), N1–C2–N3 103.5(3), C2–N3–C4 110.8(3), N3–C4–C5 107.4(3), C4–C5–N1 106.8(4), C5–N1–C2 111.5(3), C2–N1–C11 126.6(3), C2–N3–C31 127.6(3).

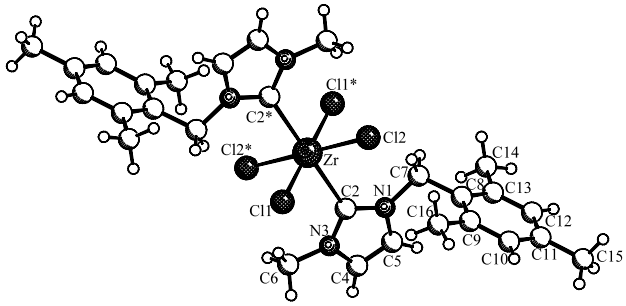

Fig. 4. Molecular structure of **4c**. Selected bond lengths (Å) and angles (°): Zr–Cl1 2.431(1), Zr–Cl2 2.436(1), Zr–C2 2.448(3), N1–C2 1.364(4), C2–N3 1.369(4), N1–C5 1.376(4), N3–C4 1.364(4), N1–C7 1.480(4), N3–C6 1.465(4), C4–C5 1.333(5); Cl1–Zr–Cl1* 180.0, Cl2–Zr–Cl2* 180.0, C2–Zr–C2* 180.0, Cl1–Zr–Cl2 88.57(4), Cl1–Zr–C2 92.34(8), Cl2–Zr–C2 92.15(7), Zr–C2–N1 128.8(2), Zr–C2–N3 127.2(2), N1–C2–N3 102.9(3), C2–N3–C4 111.5(3), N3–C4–C5 107.4(3), C4–C5–N1 106.8(3), C5–N1–C2 111.4(3), C2–N1–C7 127.0(3), C2–N3–C6 126.3(3).

carbene. In order to trace the factors causing rotational barriers of the planar five-membered heterocycle ligands in our pseudooctahedral biscarbenes Group 4 transition metal complexes with d^0 electron configuration, the most stable conformations of the complexes $\{C(N^iPr)_2(CH)_2\}_2MCl_4$ (M = Ti **6a**, Zr **4a**, Hf **5a**), and the model complex $\{C(N^iPr)(NMe)(CH)_2\}_2ZrCl_4$ (**4d**) and $\{C(NH)_2(CH)_2\}_2ZrCl_4$ (**4f**) have been first fully optimized by aid of DFT calculations. For the complexes **4**–**6a** and **4d**, two local minima were found, which correspond to the coplanar **Ia** and perpendicular **Ib** structures of the two carbene ligands as depicted in Scheme 2.

From Table 2, we can see that for **4**–**6a** and **4d** there is practically no energy difference independent of the transition metal or the substituents on the N atoms ($\Delta E < 0.4$ kcal mol^{-1}). Contrary to the experimentally determined structures, the perpendicular geometry **Ib** is slightly prefered over the coplanar structure **Ia** for **4a**–**5a** and **4d**. Surprisingly, the minima found for the H-substituted model complex **4e** differ from those observed for the other complexes. The optimized geometries can be described as the coplanar **IIa** and the perpendicular

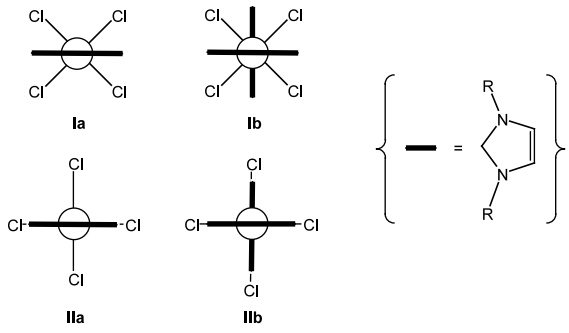

Scheme 2.

Table 2
Relative energies (kcal mol^{-1}) for the DFT calculated biscarbene-transition metal complexes **4**–**6(a)**, and model complexes **4d** and **4e**

Complex	M	R	R′	Coplanar		Perpendicular		Transition state [a]
				Ia	**IIa**	**Ib**	**IIb**	
6a	Ti	^{i}Pr	^{i}Pr	0.0		+0.2		+3.8
4a	Zr	^{i}Pr	^{i}Pr	+0.1		0.0		+2.7
5a	Hf	^{i}Pr	^{i}Pr	+0.3		0.0		+2.8
4d	Zr	^{i}Pr	Me	+0.3		0.0		+2.5
4e	Zr	H	H	– [b]	+5.6	+8.7	0.0	

[a] From a partial optimization with a dihedral angle Cl–Zr–C–N fixed at 0°.
[b] A local minimum could not be found.

Ib and **IIb** conformations of the two planar five-membered heterocyclic ligands (Scheme 2).

The most stable conformation **4e**–**IIb** corresponds to a structure in which each carbene ligand is coplanar with one $ZrCl_2$ fragment. The energy differences between the optimized structures are also larger than those calculated for the isopropyl complexes (**4a**–**6a**, **4d**). The coplanar **IIa** and perpendicular **Ib** structures are higher in energy than the most stable geometry **IIb** by 5.6 and 8.7 kcal mol^{-1}, respectively. That means that the conformation **IIb** seems to be electronically preferred, but from a steric point of view unfavorable due to steric contacts of the bulky substituents on the nitrogen atoms. The bond analysis on selected conformations of **4a** and **4e** confirms this conclusion (Table 3).

The metal carbene bond energies (BE) appear very similar with values in the range of 112–115 kcal mol^{-1}. Nevertheless, the study of the different bond energy contributions show that the steric term ΔE° is for **4e**–**Ib** more than twice as much than that of **4e**–**IIb** (−31 vs. −15 kcal mol^{-1}). On the other hand, the strongest interaction of the carbene ligands with the metal center is seen for conformation **IIb** of **4e** in terms of electrostatics ΔE_{elstat} as well as the orbital interaction ΔE_{int}. There is clearly competition between steric and electronic factors in the most stable structure of these compounds. From the above results, we can conclude that the favored **IIb** structure of the model complex **4e** is governed by electronic factors and the ground state structure found for the isopropyl complexes are dominated by steric effects.

Table 3
Metal–carbene bond energy partitioning (kcal mol^{-1}) for selected conformations of the complexes **4a**, **5a** and **4e**

Complex	**4a**–**Ib**	**5a**–**Ib**	**4e**–**Ib**	**4e**–**IIb**
M	Zr	Hf	Zr	Zr
R = R′	^{i}Pr	^{i}Pr	H	H
ΔE_{Pauli}	155	166	136	172
ΔE_{elstat}	−174	−187	−168	−187
ΔE°	−19	−21	−31	−15
ΔE_{int}	−93	−94	−82	−100
BE	112	115	114	115

In Fig. 5, we can also notice that the MX_4Y_2 model species **4e**–**IIb** is slightly distorted from the octahedral geometry. The calculated values for the bond angles Cl–Zr–C and Cl–Zr–Cl amount to 79.5 (and 100.5°) and 91.9°. Such second order Jahn–Teller type distortions have already been studied theoretically by Hoffmann and coworker [12] and Albright et al. [13] for octahedral ML_6 complexes (O_h symmetry) with preferentially low d-electron counts. One of the two typical distortional pathways is a decrease of one *trans*-L–M–L angle from 180°. This *trans* distortion happens in our complexes for each meridional (carbene) MCl_2 plane. This lowering of symmetry results in mixings out of the two sets of frontier molecular orbitals t_{2g} and t_{1u} giving rise to two new empty and higher lying M–L antibonding Φ_2 and also new occupied and lower lying M–L bonding Φ_1 hybrids (Scheme 3).

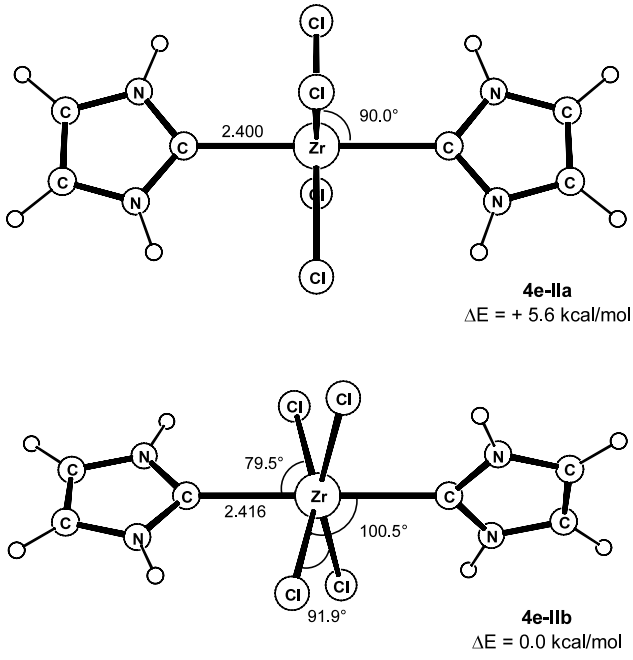

Fig. 5. Calculated structures **IIa** and **IIb** of the non-substituted model complex **4e**.

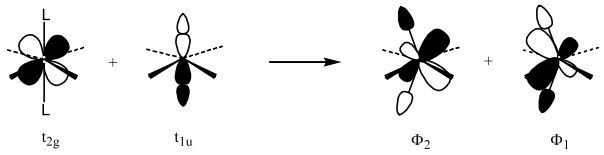

Scheme 3.

The two occupied $t_{1u} \rightarrow \Phi_1$ σ-orbital transformations are found to be quite stabilizing, since Φ_1 is in phase with σ-lobes of the chlorine substituents.

To estimate the rotational barriers of the carbene ligand, linear transit calculations were carried out on complexes **4a** and **4e** simulating the rotation of one carbene around the metal–carbon bond from the coplanar into the perpendicular model (**Ia** → **Ib** for **4a**, and **IIa** → **IIb** for **4e**). For each fixed value of α defined as the dihedral angle $N_1–C_1\cdots C_2–N_2$ (varied from 0 to 90°), the rest of the geometry was fully optimized. The potential energy surfaces as functions of the reaction coordinate α are presented in Fig. 6.

In the case of the complex **4e** in which the steric and electronic influences between the carbene ligands and the metal fragment $ZrCl_4$ are the strongest for **IIb**, the surface does not pass by a maximum during the rotation. On the other hand, the bulky isopropyl groups of **4a** get into steric contact with the chlorine ligands when the carbene cycle becomes coplanar with one $ZrCl_2$ fragment leading to the highest energy. This conformation which is the transition state along the rotational path has been determined more accurately constraining the dihedral angle N1–C1–Zr–Cl to 0° (Fig. 7).

In this way, the rotational barriers have been estimated for complexes **6a**(Ti), **4a**(Zr), **5a**(Hf), and **4d**(Zr) to only 3.8, 2.7, 2.8 and 2.5 kcal mol^{-1}, respectively.

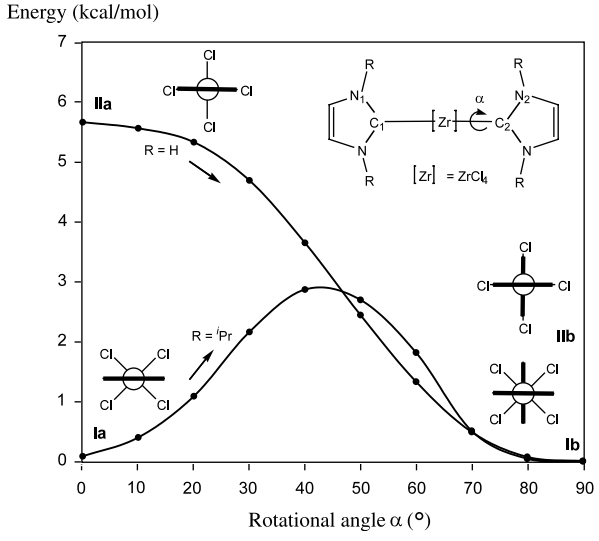

Fig. 6. Potential energy surfaces for $\{C(NR)_2(CH)_2\}_2ZrCl_4$ with R = ^{i}Pr (**4a**) and H (**4e**) showing the changes in relative energies (kcal mol^{-1}) with respect to the rotational angle α (°).

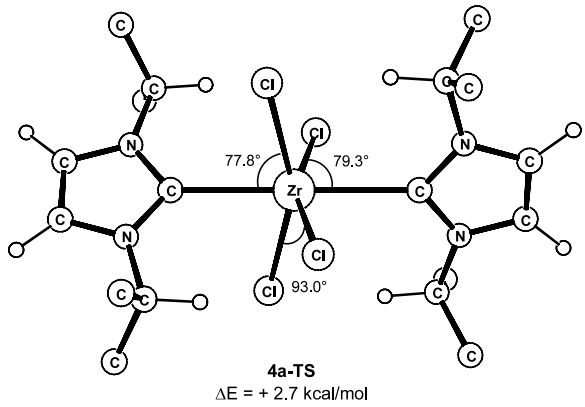

Fig. 7. Calculated rotational transition state of the zirconium complex **4a** in which the dihedral angles Cl–Zr–C–N have been fixed at 0°.

These weak energy barriers are indications for rapid rotations of the carbene ligands in solution. Electronically, this feature is largely the result of the lack of π-back bonding in the d^0 systems.

2.3. Polymerization reactions

Group 4 metallocene complexes have become of a great importance as components of homogeneous Ziegler–Natta-type olefin polymerization catalysts [14]. A variety of other systems, such as the Cp/amido Group 4 metal 'constrained geometry' catalysts have become significant for olefin copolymerization [15]. Cp-free late transition metal Ziegler–Natta catalysts are increasingly important [16], and an increasing number of catalytically active non-Cp Group 4 metal systems is emerging from the literature recently [17].

We have, therefore, briefly investigated the catalytic ethene polymerization features of the **4a**–**c**/methylalumoxane systems. The respective (Arduengo carbene)$_2ZrCl_4$ complexes were activated by treatment with a large excess methylalumoxane in toluene solution. Ethene polymerization reactions were carried out at four different temperatures between +5 and +90 °C (1 h reaction time) at 2 bar ethene pressure. Linear polyethylene was obtained in each of these experiments, but the **4**/MAO catalyst systems showed only moderate polymerization activities (see Table 4).

3. Experimental

Organic and inorganic starting materials (isopropylamine, 2-bromobutane, mesitylene, 40 wt.% glyoxal solution in water, 33 wt.% HBr–AcOH solution) were commercially available, and used without further purification. Solvents were dried over K–Na and distilled under Ar. Syntheses of the carbene ligands and the metal carbene complexes were carried out in an inert atmosphere (Ar) using a modified Schlenk technique or

Table 4
Ethene polymerization reactions using the systems **4**/MAO [a]

Precursor	T (°C)	Al–M [b] ratio	Yield (g)	Activity [a]	m.p. (°C)
4a (19 μmol)	5	1737	0.74	17	129
4a (19 μmol)	25	1737	2.69	75	128
4a (19 μmol)	60	1737	1.15	32	127
4a (15 μmol)	90	1737	1.04	29	128
4b (20 μmol)	5	1650	2.65	68	130
4b (20 μmol)	25	1650	1.48	38	126
4b (20 μmol)	60	1650	0.94	24	127
4b (20 μmol)	90	1650	0.29	7	127
4c (15 μmol)	5	2200	1.68	56	129
4c (15 μmol)	25	2200	1.40	46	129
4c (15 μmol)	60	2200	0.95	32	128
4c (15 μmol)	90	2200	0.46	15	127
5a (16 μmol)	25	2063	0.05	1	128

[a] In units of kg of polymer (mol of M [b])$^{-1}$ bar^{-1} h^{-1}.
[b] M = Zr, (**4a**–**4c**), Hf (**5a**).

glove box (< 1 ppm oxygen or moisture). The metal complexes were stored at −37 °C to prevent decomposition. Imidazolium salts were treated under Ar because of their hygroscopic behavior. For additional general information including a list of instruments used for physical and spectroscopical characterization of the compounds, see Ref. [18]. NMR assignments were usually secured by a series of 2D experiments [19]. X-ray crystal structure analyses: data sets were collected with Enraf–Nonius CAD4 and Nonius KappaCCD diffractometers, the latter one equipped with a rotating anode generator Nonius FR591. Programs used: data collection EXPRESS (Nonius B.V., 1994) and COLLECT (Nonius B.V., 1998), data reduction MOLEN (K. Fair, Enraf–Nonius B.V., 1990) and DENZO-SMN (Z. Otwinowski, W. Minor, Methods Enzymol. 276 (1997) 307–326), absorption correction for CCD data SORTAV (R.H. Blessing, Acta Crystallogr. Sect. A 51 (1995) 33–37; R.H. Blessing, J. Appl. Crystallogr. 30 (1997) 421–426), structure solution SHELXS-97 (G.M. Sheldrick, Acta Crystallogr. Sect. A 46 (1990) 467–473), structure refinement SHELXL-97 (G.M. Sheldrick, Universität Göttingen, 1997), graphics SCHAKAL (E. Keller, Universität Freiburg, 1997).

3.1. Synthesis and characterization of bis[1,3-diisopropylimidazol-2-ylidene]$ZrCl_4$ and $-HfCl_4$ (**4a**, **5a**)

3.1.1. Preparation of 1,3-diisopropylimidazolium tetraphenylborate [**2a**(BPh_4)]

A suspension of 1.00 g (5.30 mmol) 1,3-diisopropylimidazolium chloride [**2a**(Cl)] [9] and 1.81 g (5.30 mmol) sodium tetraphenylborate was stirred at room temperature (r.t.) for 18 h. The precipitate was collected by filtration and stirred in CH_2Cl_2 to dissolve the imidazolium salt. The unsoluble NaCl was filtered off, the CH_2Cl_2 was removed in vacuo, and the product dried in vacuo to yield 1.67 g (67%) of **2a**(BPh_4) as a white, hygroscopic powder. Crystals for X-ray diffraction were obtained by crystallization from CH_2Cl_2, m.p. 184 °C. Anal. Calc. for $C_{33}H_{37}BN_2$ (MW 472.5): C, 83.89; H, 7.89; N, 5.93. Found: C, 82.54; H, 7.38; N, 6.02%. ^{1}H-NMR (CH_2Cl_2-d_2, 400.1 MHz): $\delta = 7.77$ (d, $^4J_{HH} = 1.7$ Hz, 2H, 4-H, 5-H), 6.06 (t, $^4J_{HH} = 1.7$ Hz, 1H, 2-H), 3.90 (sept, $^3J_{HH} = 6.7$ Hz, 2H, N–C*H*), 1.28 (d, $^3J_{HH} = 6.7$ Hz, 12H, –CH(CH_3)$_2$); [BPh_4^-] : 7.46 (*o*-H), 7.04 (*m*-H), 6.86 (*p*-H). ^{13}C-NMR (CH_2Cl_2-d_2, 100.6 MHz): $\delta =$ 132.6 (C2), 119.4 (C4, C5), 53.2 (N–*C*H), 23.4 (–CH(*C*H$_3$)$_2$); [BPh_4^-] : 164.4 (*ipso*-C), 136.6 (*o*-C), 126.7 (*m*-C), 122.7 (*p*-C). IR (KBr): $\tilde{\nu} = 3148$ (m), 3054 (m), 2982 (m), 1549 (m), 1479 (s), 1425 (s), 1186 (s), 1148 (s), 1029 (m), 845 (m), 741 (s) cm^{-1}.

3.1.2. X-ray crystal structure analysis of **2a**(BPh_4)

Formula $C_{33}H_{37}BN_2$, $M = 472.46$, colorless crystal $0.20 \times 0.20 \times 0.20$ mm, $a = 11.251(1)$, $c = 22.855(1)$ Å, $V = 2893.1(4)$ Å^3, $\rho_{calc} = 1.085$ g cm^{-3}, $\mu = 0.62$ cm^{-1}, empirical absorption correction via SORTAV ($0.988 \leq T \leq 0.988$), $Z = 4$, tetragonal, space group $P\bar{4}2_1c$ (No. 114), $\lambda = 0.71073$ Å, $T = 198$ K, ω and φ scans, 10 238 reflections collected ($\pm h$, $\pm k$, $\pm l$), [(sin θ)/λ] = 0.68 Å^{-1}, 3581 independent ($R_{int} = 0.059$) and 2221 observed reflections [$I \geq 2\sigma(I)$], 166 refined parameters, $R = 0.048$, $wR^2 = 0.092$, max. residual electron density 0.15 (−0.22) e Å^{-3}, hydrogens calculated and refined as riding atoms.

3.1.3. Synthesis of 1,3-diisopropylimidazol-2-ylidene (**3a**)

A modified literature procedure was used for the synthesis of the stable carbene **3a** [9]. A suspension of 1,3-diisopropylimidazolium chloride (**2a**(Cl)), (7.18 g, 38.0 mmol), NaH (1.00 g, 41.8 mmol), and KO^{t}Bu (213 mg, 1.90 mmol) in 70 ml of THF was stirred for 24 h at

r.t. while a brown solution was formed. The solvent was removed in vacuo and the product distilled at 90 °C and condensated at −196 °C to yield 5.50 g (95%) of **3a** as a brown oil. ^{1}H-NMR (C_6H_6-d_6, 200.1 MHz): $\delta = 6.54$ (s, 2H, 4-H, 5-H), 4.39 (sept, $^3J_{HH} = 6.7$ Hz, 2H, N–C*H*), 1.27 (d, $^3J_{HH} = 6.7$ Hz, 12H, –CH_3). ^{13}C-NMR (C_6H_6-d_6, 50.3 MHz): $\delta = 210.5$ (C2), 115.5 (C4, C5), 51.1 (N–*C*H), 24.2 (–CH_3).

3.1.4. Preparation of bis[1,3-diisopropylimidazol-2-ylidene]zirconium-tetrachloride (**4a**)

A solution of 1,3-diisopropylimidazol-2-ylidene (**3a**) [9] (600 mg, 3.94 mmol) in 40 ml of $C_6H_5CH_3$ was added dropwise to a suspension of $ZrCl_4(thf)_2$ [21] (743 mg, 1.97 mmol) in 40 ml $C_6H_5CH_3$ at −78 °C. The reaction mixture was warmed up to 0 °C. At this temperature the $C_6H_5CH_3$ was removed in vacuo, the product was washed with cold $C_6H_5CH_3$ and C_5H_{12}, respectively, and dried in vacuo to yield 1.12 g (99%) of a beige powder. Single crystals for the X-ray crystal structure analysis were obtained from CH_2Cl_2, m.p. 167 °C. Anal. Calc. for $C_{18}H_{32}Cl_4N_4Zr$ (MW 537.5): C, 40.22; H, 6.00; N, 10.42. Found: C, 39.61; H, 6.37; N, 10.44%. ^{1}H-NMR (CH_2Cl_2-d_2, 599.9 MHz): $\delta = 7.10$ (s, 4H, 4-H, 5-H), 5.90 (sept, $^3J_{HH} = 6.6$ Hz, 4H, N–C*H*), 1.44 (d, $^3J_{HH} = 6.6$ Hz, 24H, –CH(CH_3)$_2$). ^{13}C-NMR (CH_2Cl_2-d_2, 150.8 MHz): $\delta = 181.8$ (C2), 117.4 (C4, −5), 52.2 (N–*C*H), 23.6 (–CH(*C*H_3)$_2$). IR (KBr): $\tilde{\nu} = 3136$ (m), 2975 (m), 1463 (m), 1387 (m), 1208 (s), 1022 (w), 755 (m), 509 (m) cm^{-1}.

3.1.5. X-ray crystal structure analysis of **4a**

Formula $C_{18}H_{32}Cl_4N_4Zr \cdot C_6H_6$, $M = 615.60$, colorless crystal $0.30 \times 0.10 \times 0.07$ mm, $a = 9.465(1)$, $b = 12.015(1)$, $c = 13.409(1)$ Å, $\beta = 100.38(1)°$, $V = 1499.9(2)$ Å^3, $\rho_{calc} = 1.363$ g cm^{-3}, $\mu = 7.41$ cm^{-1}, empirical absorption correction via SORTAV ($0.808 \leq T \leq 0.950$), $Z = 2$, monoclinic, space group $P2_1/n$ (No. 14), $\lambda = 0.71073$ Å, $T = 198$ K, ω and φ scans, 6240 reflections collected ($\pm h$, $\pm k$, $\pm l$), $[(\sin\theta)/\lambda] = 0.66$ Å^{-1}, 3527 independent ($R_{int} = 0.032$) and 2722 observed reflections [$I \geq 2\sigma(I)$], 155 refined parameters, $R = 0.040$, $wR^2 = 0.088$, max. residual electron density 0.65 (−0.47) e Å^{-3}, hydrogens calculated and refined as riding atoms.

3.1.6. Preparation of bis[1,3-diisopropylimidazol-2-ylidene]hafnium-tetrachloride (**5a**)

A solution of **3a** [9] (52.0 mg, 344 μmol) in 40 ml of $C_6H_5CH_3$ was added dropwise to a suspension of $HfCl_4(thf)_2$ [21] (80 mg, 172 μmol) in 40 ml $C_6H_5CH_3$ at −78 °C. The reaction mixture was allowed to warm to 0 °C. At this temperature the $C_6H_5CH_3$ was removed in vacuo, the product was washed with cold $C_6H_5CH_3$ and C_5H_{12}, respectively, and dried in vacuum to yield 99 mg (91%) of a beige powder. Single crystals for the X-ray crystal structure analysis were obtained from CH_2Cl_2, m.p. 267 °C (dec.). Anal. Calc. for $C_{18}H_{32}Cl_4HfN_4$ (MW 624.8): C, 34.60; H, 5.16; N, 8.97. Found: C, 33.93; H, 4.80; N, 8.28%. ^{1}H-NMR (CH_2Cl_2-d_2, 599.9 MHz): $\delta = 7.12$ (s, 4H, 4-H, 5-H), 5.94 (sept, $^3J_{HH} = 6.60$ Hz, 4H, N–C*H*), 1.44 (d, $^3J_{HH} = 6.60$ Hz, 24H, –CH(CH_3)$_2$). ^{13}C-NMR (CH_2Cl_2-d_2, 150.8 MHz): $\delta = 189.1$ (C2), 117.7 (C4, C-5), 52.3 (N–*C*H), 23.4 (–CH(*C*H_3)$_2$). IR (KBr): $\tilde{\nu} =$ 3174 (w), 3137 (w), 2983 (m), 2940 (w), 1563 (w), 1480 (m), 1384 (m), 1267 (m), 1206 (s), 1130 (w), 765 (m) cm^{-1}.

3.1.7. X-ray crystal structure analysis of **5a**

Formula $C_{18}H_{32}Cl_4HfN_4 \cdot CH_2Cl_2$, $M = 709.69$, colorless crystal $0.40 \times 0.15 \times 0.15$ mm, $a = 9.405(1)$, $b = 11.444(1)$, $c = 13.869(1)$ Å, $\beta = 100.17(1)°$, $V = 1469.3(2)$ Å^3, $\rho_{calc} = 1.604$ g cm^{-3}, $\mu = 41.09$ cm^{-1}, empirical absorption correction via SORTAV ($0.290 \leq T \leq 0.578$), $Z = 2$, monoclinic, space group $P2_1/n$ (No. 14), $\lambda = 0.71073$ Å, $T = 198$ K, ω and φ scans, 6083 reflections collected ($\pm h$, $\pm k$, $\pm l$), $[(\sin\theta)/\lambda] = 0.66$ Å^{-1}, 3403 independent ($R_{int} = 0.016$) and 2770 observed reflections [$I \geq 2\sigma(I)$], 156 refined parameters, $R = 0.020$, $wR^2 = 0.049$, max. residual electron density 0.51 (−1.00) e Å^{-3}, hydrogens calculated and refined as riding atoms.

3.2. Synthesis and characterization of bis[1-methyl-3-(1-methylpropyl)imidazol-2-ylidene]$ZrCl_4$ (**4b**)

3.2.1. Preparation of 1-methyl-3-(1-methylpropyl)imidazolium bromide [**2b**(Br)]

A solution of 2-bromobutane (8.34 g, 60.9 mmol) in 10 ml of EtOAc was added to a solution of 1-methylimidazole (5.00 g, 60.9 mmol) in 10 ml of EtOAc. The reaction mixture was stirred under reflux for 4 h. During this time a beige solid was precipitated. The solvent was decanted and the remaining solid washed with EtOAc (3×10 ml) at reflux temperature. The product was dried in vacuo to yield 4.89 g (43%) of the hygroscopic, waxy product **2b**(Br), m.p. 74 °C. Anal. Calc. for $C_8H_{15}BrN_2$ (MW 219.1): C, 43.85; H, 6.90; N, 12.78. Found: C, 43.27; H, 7.28; N, 12.89%. ^{1}H-NMR ($CHCl_3$-d_1, 400.1 MHz): $\delta = 10.2$ (s, 2H, 2-H), 7.47 (d, $^3J_{HH} = 1.8$ Hz, 1H, 4-H), 7.33 (d, $^3J_{HH} = 1.8$ Hz, 1H, 5-H), 4.41 (m, 1H, 6-H), 3.94 (s, 3H, N–CH_3), 1.76 (m, 2H, 7-H), 1.40 (d, $^3J_{HH} = 6.8$ Hz, 3H, 6-CH_3), 0.71 (t, $^3J_{HH} = 7.3$ Hz, 3H, 8-H). ^{13}C-NMR ($CHCl_3$-d_1, 100.6 MHz): $\delta = 136.4$ (C2), 123.8 (C4), 120.2 (C5), 58.8 (C6), 36.6 (N–*C*H_3), 29.9 (C7), 20.8 (6-*C*H_3), 10.1 (C8). IR (KBr): $\tilde{\nu} = 3064$ (s), 2981 (s), 1584 (m), 1467 (m), 1177 (s), 675 (w), 765 (m), 634 (m). MS (ESI): $m/z = 139.2$ [M^+].

*3.2.2. X-ray crystal structure analysis of **2b**(BPh_4)*

For characterization by X-ray diffraction the anion was exchanged by treatment with $NaBPh_4$ (for details see Section 4). Single crystals were obtained from CH_2Cl_2.

Formula $C_{32}H_{35}BN_2$, $M = 458.43$, light yellow crystal $0.50 \times 0.20 \times 0.15$ mm, $a = 11.581(1)$, $b = 15.146(2)$, $c = 31.327(1)$ Å, $V = 5494.9(9)$ Å^3, $\rho_{calc} = 1.108$ g cm^{-3}, $\mu = 4.79$ cm^{-1}, no absorption correction ($0.796 \leq T \leq 0.932$), $Z = 8$, orthorhombic, space group $C222_1$ (No. 20), $\lambda = 1.54178$ Å, $T = 223$ K, ω–2θ scans, 3099 reflections collected ($+h$, $-k$, $+l$), $[(\sin\theta)/\lambda] = 0.66$ Å^{-1}, 3099 independent and 2578 observed reflections [$I \geq 2\sigma(I)$], 321 refined parameters, $R = 0.065$, $wR^2 = 0.191$, max. residual electron density 0.45 (-0.29) e Å^{-3}, hydrogens calculated and refined as riding atoms.

*3.2.3. Synthesis of 1-methyl-3-(1-methylpropyl)imidazol-2-ylidene (**3b**)*

A modified literature procedure [9] was used for the synthesis of the *Arduengo* carbene **3b**. A suspension of **2b**(Br) (4.81 g, 21.9 mmol), NaH (600 mg, 25.0 mmol), and KO^{t}Bu (128 mg, 1.14 mmol) in 50 ml of THF was stirred for 24 h at r.t. During this time a yellow solution was formed. The solvent was removed in vacuo and the product distilled at 90 °C and condensated at −196 °C to yield 1.97 g (65%) of **3b** as a yellow oil. ^{1}H-NMR (C_6H_6-d_6, 400.1 MHz): $\delta = 6.46$ (d, $^3J_{HH} = 1.4$ Hz, 1H, 5-H), 6.38 (d, $^3J_{HH} = 1.4$ Hz, 1H, 4-H), 4.11 (m, 1H, 6-H), 3.40 (s, 3H, N–CH_3), 1.55 (m, 2H, 7-H), 1.27 (d, $^3J_{HH} = 6.8$ Hz, 3H, 6-CH_3), 0.75 (t, $^3J_{HH} = 7.2$ Hz, 3H, 8-H). ^{13}C-NMR (C_6H_6-d_6, 100.6 MHz): $\delta = 215.6$ (C2), 120.7 (C4), 117.7 (C5), 59.1 (C6), 38.2 (N–CH_3), 32.2 (C7), 23.6 (6-CH_3), 12.0 (C8).

*3.2.4. Preparation of bis[1-methyl-3-(1-methylpropyl)imidazol-2-ylidene]$ZrCl_4$ (**4b**)*

A solution of **3b** (79.0 mg, 0.57 mmol) in 40 ml of $C_6H_5CH_3$ was added dropwise to a suspension of $ZrCl_4(thf)_2$ [21] (108 mg, 0.29 mmol) in 40 ml of $C_6H_5CH_3$ at −78 °C. The reaction mixture was warmed up to 0 °C. At this temperature the $C_6H_5CH_3$ was removed in vacuo, the product was washed with cold $C_6H_5CH_3$ and C_5H_{12}, respectively, and dried in vacuo to yield 130 mg (89%) of a beige powder. Single crystals for the X-ray crystal structure analysis were obtained from CH_2Cl_2, m.p. 153 °C (254 °C dec.). Anal. Calc. for $C_{16}H_{28}Cl_4N_4Zr$ (MW 509.5): C, 37.72; H, 5.54; N, 11.00. Found: C, 37.17; H, 5.77; N, 10.63%. ^{1}H-NMR (CH_2Cl_2-d_2, 599.9 MHz): $\delta = 7.02$ (d, $^3J_{HH} = 1.8$ Hz, 2H, 5-H), 6.97 (d, $^3J_{HH} = 1.8$ Hz, 2H, 4-H), 5.59 (m, 2H, 6-H), 4.13 (s, 6H, N–CH_3), 1.78 (m, 4H, 7-H), 1.42 (d, $^3J_{HH} = 6.6$ Hz, 6H, 6-CH_3), 0.95 (t, $^3J_{HH} = 7.2$ Hz, 3H, 8-H). ^{13}C-NMR (CH_2Cl_2-d_2, 150.8 MHz): $\delta =$ 183.5 (C2), 123.6 (C4), 116.8 (C5), 57.3 (C6), 40.1 (N–CH_3), 31.2 (C7), 21.2 (6-CH_3), 10.6 (C8). IR (KBr): $\tilde{\nu} =$ 3140 (m), 2964 (m), 1708 (w), 1660 (m), 1591 (w), 1550 (w), 1453 (m), 1262 (s), 1095 (vs), 1026 (vs), 803 (vs), 669 (w), 623 (m).

*3.2.5. X-ray crystal structure analysis of **4b***

Formula $C_{16}H_{28}Cl_4N_4Zr$, $M = 509.44$, colorless crystal $0.10 \times 0.10 \times 0.03$ mm, $a = 15.055(1)$, $b = 9.675(1)$, $c = 16.669(1)$ Å, $\beta = 114.81(1)°$, $V = 2203.9(3)$ Å^3, $\rho_{calc} = 1.535$ g cm^{-3}, $\mu = 9.91$ cm^{-1}, empirical absorption correction via SORTAV ($0.907 \leq T \leq 0.971$), $Z = 4$, monoclinic, space group $C2/c$ (No. 15), $\lambda = 0.71073$ Å, $T = 198$ K, ω and φ scans, 4543 reflections collected ($\pm h$, $\pm k$, $\pm l$), $[(\sin\theta)/\lambda] = 0.67$ Å^{-1}, 2720 independent ($R_{int} = 0.027$) and 2183 observed reflections [$I \geq 2\sigma(I)$], 118 refined parameters, $R = 0.045$, $wR^2 = 0.099$, max. residual electron density 1.35 (-0.61) e Å^{-3}, hydrogens calculated and refined as riding atoms.

*3.3. Synthesis and characterization of bis[1-methyl-3-(2,4,6-trimethylbenzyl)-imidazol-2-ylidene]$ZrCl_4$ (**4c**)*

3.3.1. Synthesis of 1-(bromomethyl)-2,4,6-trimethylbenzene [20]

A 33 wt.% HBr–AcOH solution (19 ml) was rapidly added to a mixture of mesitylene (12.0 g, 0.10 mol), paraformaldehyde (3.08 g, 0.10 mol), and 50 ml of glacial AcOH. The mixture was kept at 40–50 °C for 2 h and then poured into 100 ml of water. The product was collected by filtration and dried in vacuo to yield 18.1 g (85%) of a white powder. ^{1}H-NMR ($CHCl_3$-d_1, 200.1 MHz): $\delta = 6.88$ (s, 2H, aryl–H), 4.60 (s, 2H, CH_2Br), 2.42 (s, 6H, 2-, 6-CH_3), 2.30 (s, 3H, 4-CH_3). ^{13}C-NMR ($CHCl_3$-d_1, 50.3 MHz): $\delta = 138.4$ (C-4), 137.3 (C-2, -6), 131.0 (C-1), 129.3 (C-3, -5), 29.6 (CH_2Br), 21.0 (4-CH_3), 19.1 (2-, 6-CH_3).

*3.3.2. Synthesis of 1-methyl-3-(2,4,6-trimethylbenzyl)imidazolium bromide [**2c**(Br)]*

1-Methylimidazole (2.00 g, 24.4 mmol) was added rapidly to a solution of 1-(bromomethyl)-2,4,6-trimethylbenzene (5.22 g, 22.4 mmol) in 200 ml of EtOAc. Immediately, a voluminous white solid precipitated. The reaction mixture was stirred under reflux for additional 5 min, then the product was collected by filtration, washed with EtOAc, and dried in vacuum to yield 5.90 g (81%) of **2c**(Br) as a white, hygroscopic powder. Crystals for X-ray crystal structure analysis were obtained from the mother liquor, m.p. 185 °C. Anal. Calc. for $C_{14}H_{19}BrN_2$ (MW 295.3): C, 56.96; H, 6.49; N, 9.49. Found: C, 56.50; H, 6.71; N, 9.17%. ^{1}H-NMR ($CHCl_3$-d_1, 400.1 MHz): $\delta = 10.1$ (s, 1H, 2-CH), 7.60 (d, $^3J_{HH} = 1.8$ Hz, 1H, 4-CH), 6.86 (d, $^3J_{HH} = 1.8$ Hz, 1H, 5-CH), 6.84 (s, 2H, *m*-phenyl–H), 5.47 (s, 2H, –CH_2), 4.05 (s, 3H, N–CH_3), 2.20 (s, 9H, *o*-, *p*-CH_3). ^{13}C-NMR ($CHCl_3$-d_1, 100.6 MHz): $\delta = 138.6$ (*ipso*-*C*), 136.7 (C2), 135.7 (*o*-C), 128.6 (phenyl–CH), 123.9 (C4),

122.6 (C5), 119.4 (*p*-C), 46.6 ($-CH_2$), 35.7 (N–CH_3), 19.6 (*p*-CH_3), 18.5 (*o*-CH_3). IR (KBr): $\tilde{\nu} = 3147$ (m), 3071 (m), 1636 (m), 1577 (m), 1463 (m), 1281 (w), 1158 (s), 1096 (w), 1033 (w), 882 (w), 847 (w), 799 (m), 758 (w), 669 (w), 621 (m).

3.3.3. X-ray crystal structure analysis of **2c**(Br)

Formula $C_{14}H_{19}BrN_2 \cdot H_2O$, $M = 313.24$, colorless crystal $0.35 \times 0.25 \times 0.05$ mm, $a = 12.595(1)$, $b = 9.743(1)$, $c = 13.230(1)$ Å, $\beta = 109.31(1)^\circ$, $V = 1532.2(2)$ Å^3, $\rho_{calc} = 1.358$ g cm^{-3}, $\mu = 35.82$ cm^{-1}, empirical absorption correction via ψ scan data ($0.367 \le T \le 0.841$), $Z = 4$, monoclinic, space group $P2_1/n$ (No. 14), $\lambda = 1.54178$ Å, $T = 223$ K, ω–2θ scans, 3259 reflections collected ($-h$, $+k$, $\pm l$), $[(\sin\theta)/\lambda] = 0.62$ Å^{-1}, 3117 independent ($R_{int} = 0.035$) and 2710 observed reflections [$I \ge 2\sigma(I)$], 164 refined parameters, $R = 0.036$, $wR^2 = 0.102$, max. residual electron density 0.29 (-0.58) e Å^{-3}, hydrogens calculated and refined as riding atoms.

3.3.4. Synthesis of 1-methyl-3-(2,4,6-trimethylbenzyl)imidazol-2-ylidene (**3c**)

A suspension of 1-methyl-3-(2,4,6-trimethylbenzyl)-imidazolium bromide (3.00 g, 10.1 mmol), and NaH (0.40 g, 16.7 mmol) in 60 ml of THF was stirred for 16 h at r.t. The resulting NaBr precipitate was filtered off, the THF solvent was removed in vacuo, and the product was dried in vacuo to yield 1.87 g (86%) of a yellow solid, m.p. 88 °C (117 °C dec.). ^{1}H-NMR (C_6H_6-d_6, 599.9 MHz): $\delta = 6.70$ (s, 2H, *m*-aryl–H), 6.34 (d, $^3J_{HH} = 1.8$ Hz, 1H, 5-H), 6.22 (d, $^3J_{HH} = 1.8$ Hz, 1H, 4-H), 5.20 (s, 2H, $-CH_2$), 3.39 (s, 3H, N–CH_3), 2.23 (s, 6H, *o*-CH_3), 2.09 (s, 3H, *p*-CH_3). ^{13}C-NMR (C_6H_6-d_6, 150.8 MHz): $\delta = 216.6$ (C2), 137.9 (*o*-C), 137.3 (*p*-C), 131.6 (*ipso*-C), 129.5 (*m*-C), 119.3 (C4), 117.9 (C5), 48.7 ($-CH_2$), 37.6 (N–CH_3), 20.9 (*p*-CH_3), 20.0 (*o*-CH_3). IR (KBr): $\tilde{\nu} = 2954$ (s), 1680 (s), 1625 (w), 1584 (w), 1467 (s), 1405 (w), 1364 (w), 1219 (m), 1040 (m), 868 (m), 820 (m), 765 (m), 730 (m), 669 (w).

3.3.5. Preparation of bis[1-methyl-3-(2,4,6-trimethylbenzyl)imidazol-2-ylidene]$ZrCl_4$ (**4c**)

A solution of **3c** (900 mg, 4.18 mmol) in 40 ml of $C_6H_5CH_3$ was added dropwise to a suspension of $ZrCl_4(thf)_2$ [21] (788 mg, 2.09 mmol) in 40 ml of $C_6H_5CH_3$ at -78 °C. The reaction mixture was allowed to warm to 0 °C. At this temperature volatiles were removed in vacuo, the product was washed with cold $C_6H_5CH_3$, then C_5H_{12}, and dried in vacuo to yield 2.60 g (94%) of **4c** as a beige colored powder. Single crystals for the X-ray crystal structure analysis were obtained from CH_2Cl_2, m.p. 220 °C (dec.). Anal. Calc. for $C_{28}H_{36}Cl_4N_4Zr$ (MW 661.7): C, 50.83; H, 5.48; N, 8.47. Found: C, 50.76; H, 6.12; N, 7.63%. ^{1}H-NMR (C_6H_6-d_6, 599.9 MHz): $\delta = 6.60$ (s, 4H, *m*-aryl–H), 6.25 (s, 4H, $-CH_2$), 5.89 (d, $^3J_{HH} = 1.8$ Hz, 2H, 5-H), 5.66 (d, $^3J_{HH} = 1.8$ Hz, 2H, 4-H), 3.97 (s, 6H, N–CH_3), 2.10 (s, 12H, *o*-CH_3), 2.03 (s, 6H, *p*-CH_3). ^{13}C-NMR (C_6H_6-d_6, 150.8 MHz): $\delta = 185.4$ (C2), 138.9 (*o*-C), 138.2 (*p*-C), 129.6 (*m*-C), 129.4 (*ipso*-C), 121.4 (C4), 118.2 (C5), 50.9 ($-CH_2$), 40.0 (N–CH_3), 20.9 (*p*-CH_3), 19.8 (*o*-CH_3). IR (KBr): $\tilde{\nu} = 3140$ (m), 2964 (m), 1612 (m), 1584 (m), 1467 (s), 1267 (s), 1157 (s), 1033 (m), 868 (m), 813 (m), 751 (s), 627 (w). MS (EI-ionization): $m/z = 663$ [M^+], 441.3, 281.1, 207.0, 82.0.

3.3.6. X-ray crystal structure analysis of **4c**

Formula $C_{28}H_{36}Cl_4N_4Zr$, $M = 661.63$, yellow crystal $0.15 \times 0.15 \times 0.05$ mm, $a = 12.779(1)$, $b = 14.503(1)$, $c = 8.299(1)$ Å, $\beta = 101.35(1)^\circ$, $V = 1508.0(2)$ Å^3, $\rho_{calc} = 1.457$ g cm^{-3}, $\mu = 7.43$ cm^{-1}, empirical absorption correction via SORTAV ($0.897 \le T \le 0.964$), $Z = 2$, monoclinic, space group $P2_1/c$ (No. 14), $\lambda = 0.71073$ Å, $T = 198$ K, ω and φ scans, 9721 reflections collected ($\pm h$, $\pm k$, $\pm l$), $[(\sin\theta)/\lambda] = 0.66$ Å^{-1}, 3578 independent ($R_{int} = 0.057$) and 2510 observed reflections [$I \ge 2\sigma(I)$], 173 refined parameters, $R = 0.060$, $wR^2 = 0.100$, max. residual electron density 0.41 (-0.46) e Å^{-3}, hydrogens calculated and refined as riding atoms.

3.4. Computational details

The density functional calculations utilized the ADF program package, version 2000.02 [22]. Energies and geometries were evaluated by using the local exchange-correlation potential by Vosko et al. [23], augmented in a self-consistent manner with Becke's [24] exchange gradient correction and Perdew's [25] correlation gradient correction. The standard double ξ STO basis including one polarization function was applied for the H, C, N and Cl atoms (ADF database III), whereas the triple ξ STO basis sets plus polarization were employed for the Ti, Zr and Hf transition metals (ADF database IV). The frozen core approximation was applied for the 1s electrons of C and N atoms, for the 1s–2p electrons of the Cl atoms, for the 1s–3p (Ti), 1s–3d (Zr), and 1s–4f (Hf) electrons of the transition metals. The rotational analyses simulating the rotation of one carbene around the metal–carbon bond were performed by linear transit calculations. For each fixed value of the reaction coordinate α defined as the dihedral angle N1–C1···C2–N2, all other structural parameters were fully optimized. The bonding energies BE have been calculated as the differences between total energies of the molecule and appropriate fragments (MCl_4 vs. heterocycles) at their positions in the molecule.

$$BE = -[\Delta E^\circ + \Delta E_{int}] \quad (1)$$

$$\Delta E^\circ = \Delta E_{elstat} + \Delta E_{Pauli} \quad (2)$$

This energy can be broken down in terms of orbital interactions ΔE_{int} and steric contributions ΔE°, the latter containing a component due to Pauli or exchange

repulsion as well as an electrostatic component ΔE_{elstat} (Eqs. (1) and (2)) [26].

3.5. Polymerization reactions

Polymerizations were carried out in an 1 l glass autoclave charged with 200 ml of $C_6H_5CH_3$ and 20 ml of methylalumoxane (10.5 wt.% in $C_6H_5CH_3$). At the respective temperature the stirred (600 rpm) mixture was saturated for 45 min with ethylene at a pressure of 2 bar. The catalyst precursors (ca. 10 mg) were injected (solution in CH_2Cl_2), and the polymerization reactions were carried out for 60 min under a constant pressure of ethylene (2 bar). The reaction mixture was cautiously hydrolyzed with a 1:1 mixture of MeOH and 2 N HCl. The polymer was filtered off, washed with 100 ml of 6 N HCl, and dried under vacuum for at least 3 days.

4. Supplementary material

Crystallographic data for the X-ray crystal structure analyses have been deposited with the Cambridge Crystallographic Data Centre, CCDC nos. 186402–186408 for compounds **4a**, **5a**, **4b**, **4c**, **2a**(BPh_4), **2c**(Br), and **2b**(BPh4), respectively. Copies of this information may be obtained free of charge from The Director, CCDC, 12 Union Road, Cambridge CB2 1EZ, UK (Fax: +44-1223-336033; e-mail: deposit@ccdc.cam.ac.uk or www: http://www.ccdc.cam.ac.uk). Additional spectroscopic data of the compounds described in this paper and further details on the theoretical investigation are also available.

Acknowledgements

Financial support from the Fonds der Chemischen Industrie and the Deutsche Forschungsgemeinschaft is gratefully acknowledged. Collaboration under the COST project D-12/0016/98 is acknowledged.

References

[1] A.J. Arduengo, III, Acc. Chem. Res. 32 (1999) 913.
[2] Other reviews: (a) W.A. Herrmann, C. Köcher, Angew. Chem. 109 (1997) 2256; Angew. Chem. Int. Ed. Engl. 36 (1997) 2162;
(b) T. Weskamp, P.W. Böhm, W.A. Herrmann, J. Organomet. Chem. 600 (2000) 39;
(c) W.A. Herrmann, Angew. Chem. 114 (2002) 1342; Angew. Chem. Int. Ed. Engl. 41 (2002) 1290;
(d) See also: D. Bourissou, O. Guerret, F.P. Gabbaï, G. Bertrand, Chem. Rev. 100 (2000) 39.
[3] (a) H. Stetter, H. Kuhlmann, Chem. Ber. 109 (1976) 2890;
(b) H. Stetter, A. Mertens, Liebigs Ann. Chem. (1981) 1550.
[4] For reactions of Arduengo carbenes with non-metallic substrates see e.g.: (a) N. Burford, T.S. Cameron, D.J. LeBlanc, A.D. Phillips, T.E. Concolino, K.-C. Lam, A.L. Rheingold, J. Am. Chem. Soc. 122 (2000) 5413;
(b) X. Zheng, G.E. Herberich, Organometallics 19 (2000) 375;
(c) S.B. Clendenning, P.B. Hitchcock, J.F. Nixon, L. Nyulaszi, Chem. Commun. (2000) 1305;
(d) F.E. Hahn, L. Wittenbecher, D. Le Van, R. Fröhlich, B. Wibbeling, Angew. Chem. 112 (2000) 2393; Angew. Chem. Int. Ed. Engl. 39 (2000) 2307;
(e) F.E. Hahn, D. Le Van, M.C. Moyes, T. von Fehren, R. Fröhlich, E.-U. Würthwein, Angew. Chem. 113 (2001) 3241; Angew. Chem. Int. Ed. Engl. 40 (2001) 3144.
[5] M. Niehues, G. Erker, G. Kehr, P. Schwab, R. Fröhlich, O. Blacque, H. Berke, Organometallics 21 (2002) 2905.
[6] (a) W.A. Herrmann, K. Öfele, M. Elison, F.E. Kühn, P.W. Roesky, J. Organomet. Chem. 480 (1994) C7;
(b) N. Kuhn, T. Kratz, D. Bläser, R. Boese, Inorg. Chim. Acta 238 (1995) 179.
[7] The structures of the Ti(II) complex $Cp_2Ti(CO)$(tetramethylimidazol-2-ylidene) and of $TiCl_4$(1,3-dimesityl-imidazol-2-ylidene)$_2$ are shown on Professor Arduengo's website.
[8] For examples of other types of Group 4 metal carbene complexes see e.g.: (a) P.T. Barger, B.D. Santarsiero, J. Armantrout, J.E. Bercaw, J. Am. Chem. Soc. 106 (1984) 178;
(b) J.D. Meinhart, E.V. Anslyn, R.H. Grubbs, Organometallics 8 (1989) 583;
(c) M.D. Fryzuk, S.S.H. Mao, M.J. Zaworotko, L.R. MacGillivray, J. Am. Chem. Soc. 115 (1993) 5336;
(d) Review: R. Beckhaus, Angew. Chem. 109 (1997) 694; Angew. Chem. Int. Ed. Engl. 36 (1997) 686.
[9] (a) A.J. Arduengo, III, R.L. Harlow, M. Kline, J. Am. Chem. Soc. 113 (1991) 361;
(b) A.J. Arduengo, III, H.V.R. Dias, R.L. Harlow, M. Kline, J. Am. Chem. Soc. 114 (1992) 5530;
(c) W.A. Herrmann, C. Köcher, L.J. Gooßen, G.R.J. Artus, Chem. Eur. J. 2 (1996) 1627.
[10] A.J.C. Wilson (Ed.), International Tables for Crystallography, vol. C, Kluwer Academic Publishers, Dordrecht, 1995, p. 720.
[11] A.G. Orpen, L. Brammer, F.H. Allen, O. Kennard, D.G. Watson, R. Taylor, J. Chem. Soc. Dalton Trans. (1989) S 1.
[12] P. Kubacek, R. Hoffmann, J. Am. Chem. Soc. 103 (1981) 4320.
[13] T.A. Albright, J.K. Burdett, M.-H. Whangbo, Orbital Interactions in Chemistry, Wiley, New York, 1985, p. 289.
[14] Review: (a) H.-H. Brintzinger, D. Fischer, R. Mülhaupt, B. Rieger, R.M. Waymouth, Angew. Chem. 107 (1995) 1255;
(b) H.-H. Brintzinger, D. Fischer, R. Mülhaupt, B. Rieger, R.M. Waymouth, Angew. Chem. Int. Ed. Engl. 34 (1995) 1143.
[15] A.L. McKnight, R.M. Waymouth, Chem. Rev. 98 (1998) 2587 (Review).
[16] (a) G.J.P. Britovsek, V.C. Gibson, D.F. Wass, Angew. Chem. 111 (1999) 448; Angew. Chem. Int. Ed. Engl. 38 (1999) 428;
(b) S.D. Ittel, L.K. Johnson, M. Brookhart, Chem. Rev. 100 (2000) 1169.
[17] Recent examples: (a) J. Strauch, T.H. Warren, G. Erker, R. Fröhlich, P. Saarenketo, Inorg. Chim. Acta 300–302 (2000) 810;
(b) R.J. Keaton, K.C. Jayaratne, J.C. Fettinger, L.R. Sita, J. Am. Chem. Soc. 122 (2000) 12909;
(c) J. Tian, G.W. Coates, Angew. Chem. 112 (2000) 3772; Angew. Chem. Int. Ed. Engl. 39 (2000) 3626;
(d) J. Saito, M. Mitani, J.-I. Mohri, Y. Yoshida, S. Matsui, S.-I. Ishii, S.-I. Kojoh, N. Kashiwa, T. Fujita, Angew. Chem. 133 (2001) 3002; Angew. Chem. Int. Ed. Engl. 40 (2001) 2918;
(e) J.E. Kickham, F. Guérin, J.C. Stewart, E. Urbanska, D.W. Stephan, Organometallics 20 (2001) 1175;
(f) A.P. Duncan, S.M. Mullins, J. Arnold, R.G. Bergman, Organometallics 20 (2001) 1808.
[18] D. Vagedes, G. Erker, R. Fröhlich, J. Organomet. Chem. 641 (2002) 148.

[19] S. Braun, H.-O. Kalinowski, S. Berger, 150 and More Basic NMR Experiments (and references cited therein), VCH, Weinheim, 1998.
[20] A.W. van der Made, R.H. van der Made, J. Org. Chem. 58 (1993) 1262.
[21] L.E. Manzer, Inorg. Synth. 21 (1985) 135.
[22] (a) E.J. Baerends, P. Ros, Chem. Phys. 8 (1975) 241;
(b) L. Versluis, T. Ziegler, J. Chem. Phys. 88 (1988) 322;
(c) G. te Velde, E.J. Baerends, J. Comp. Phys. 99 (1992) 84;
(d) C. Guerra, J.G. Snijders, G. te Velde, E.J. Baerends, Theor. Chem. Acc. 99 (1998) 391.
[23] S.H. Vosko, M. Wilk, M. Nusair, Can. J. Phys. 58 (1980) 1200.
[24] A.D. Becke, Phys. Rev. A 38 (1988) 3098.
[25] J.P. Perdew, Phys. Rev. B 33 (1986) 8822.
[26] (a) H.-B. Kraatz, H. Jacobsen, T. Ziegler, P.M. Boorman, Organometallics 12 (1993) 76;
(b) H. Jacobsen, T. Ziegler, Comments Inorg. Chem. 17 (1995) 301;
(c) F.M. Bickelhaupt, E.J. Baerends, Rev. Comp. Ch. 15 (2000) 1.